Klyatskina, E.; Espinosa Fernandez, L.; Darut, G.; Segovia López, EF.; Salvador Moya, MD.; Montavon, G.; Agorges, H. (2015). Sliding Wear Behavior of Al2O3-TiO2 Coatings Fabricated by the Suspension Plasma Spraying Technique. Tribology Letters. 59(1):1-9. doi:10.1007/s11249-015-0530-5.

Tribology Letters

Sliding wear behavior of Al2O3-TiO2 coatings fabricated by Suspension Plasma Spraying technique

--Manuscript Draft--

Manuscript Number:	
Full Title:	Sliding wear behavior of Al2O3-TiO2 coatings fabricated by Suspension Plasma Spraying technique
Article Type:	Article
Keywords:	Al2O3-TiO2; Nanoestructured coating; Sliding Wear; Suspension plasma spraying
Corresponding Author:	Elizaveta Klyatskina SPAIN
Corresponding Author Secondary Information:	
Corresponding Author's Institution:	
Corresponding Author's Secondary Institution:	
First Author:	Elizaveta Klyatskina
First Author Secondary Information:	
Order of Authors:	Elizaveta Klyatskina
	Lissette Espinosa-Fernández
	Geoffrey Darut
	Maria Dolores Salvador
	Francisco Segovia
	Ghislain Montavon
	Héléne Ageorges
Order of Authors Secondary Information:	
Abstract:	In this study, friction and dry sliding wear behavior of alumina and alumina-titania near-nanometric coatings have been studied. Coatings were obtained by Suspension Plasma Spraying (SPS) technique. Dry sliding wear tests were performed in an a tribometer with a ball on disk configuration, using a Al2O3 ball as a counterpart with a normal load of 2N, a sliding distance of 1200m and a sliding speed of 0.1 m/s. The influence of TiO2 addition in fabricated coatings was related with friction coefficient behavior, wear rates and wear damage patterns. A remarkable increment in wear resistance was founded by the TiO2 addition effect, in 2.6 times for the biggest amount. The analysis of wear surface was correlated with microstructural parameters, mechanical properties and wear rates.
Suggested Reviewers:	Luca LUSVARGHI Università degli Studi di Modena e Reggio Emilia luca.lusvarghi@unimore.it
	Pierre Fauchais Laboratoire Sciences des Procédés Céramiques et de Traitements de Surface (SPCTS), Faculty of Sciences, University of Limoges, fauchais@unilim.fr
	Vladimir Chirvony Universitat de Valencia, Instituto Universitario de Ciencia de los Materiales (ICMUV) vladimir.chyrvony@uv.es

Sliding wear behavior of Al_2O_3-TiO_2 coatings fabricated by Suspension Plasma Spraying technique

E. Klyatskina[1], L. Espinosa-Fernández[1], G. Darut[2], F. Segovia[1], M. D. Salvador[1], G. Montavon[2], H. Agorges[3]

[1] Instituto de Tecnología de Materiales (ITM). Universidad Politécnica de Valencia. Camino de Vera, s/n, 46022 Valencia, Spain

[2]LERMPS-EA3316, Université de Technologie de Belfort-Montbéliard, site de Sévenas, 90010 Belfort Cedex, France

[3] SPCTS-UMR CNRS 6638, Faculty of Sciences and Technologies, University of Limoges, 123 Avenue Albert Thomas, 87060 Limoges cedex, France.

Corresponding Author:

Name: Elizaveta Klyatskina

Phone: +34 660806113

E-mail: elkl1@upvnet.upv.es

Postal Address:

Instituto de Tecnología de Materiales.

Universidad Politécnica de Valencia.

Camino de Vera s/n. CP-46022

Valencia, Spain.

ABSTRACT.

In this study, friction and dry sliding wear behavior of alumina and alumina-titania near- nanometric coatings have been examined. Coatings were obtained by the Suspension Plasma Spraying (SPS) technique. Dry sliding wear tests were performed in a tribometer with ball on disk configuration, using an Al_2O_3 ball as a counterpart material with a normal load of 2N, a sliding distance of 1200 m and a sliding speed of 0.1 m/s. The influence of TiO_2 addition in fabricated coatings was linked with friction coefficient behavior, wear rates and wear damage patterns. A remarkable increase in wear resistance was found by the addition of TiO_2, 2.6 times for 40 wt.% of TiO_2. The analysis of the wear surface was correlated with microstructural parameters, mechanical properties and wear rates.

Keywords: Al_2O_3-TiO_2; Nanoestructured coating; Sliding Wear; Suspension plasma spraying

1. Introduction

Conventional Al_2O_3-TiO_2 coatings are commonly used in machine parts in order to improve resistance to wear, corrosion, oxidation, erosion and heat [1-3]. Mechanical properties such as crack resistance, adhesion strength, spallation resistance and wear resistance could be enhanced in nanostructured Al_2O_3-TiO_2 coatings [4]. Shipping, textile, machinery and printing industries may benefit from nanostructure coating applications [5-7].

Presently, a reduction of coating material particles size to nanoscale range constitutes the aim of many investigations [4, 6-12]. However, several limitations still remain in nanostructure coatings when they are manufactured directly from nano-powders, i.e. low fluidity and tendency to powder agglomeration, high reactivity and growth rates of nano-particles.

Different processes can be used to produce nanostructure coatings: atmospheric plasma spraying (APS), HVOF, flame or cold-gas spray. However, Suspension Plasma Spraying (SPS) is one of the more widely used processes to produce finely structured coatings whilst maintaining the versatility and flexibility of the thermal spray routes. SPS allows the direct injection of sub-micrometer to nanometer-sized particles by the use of liquid as a carrier medium for the suspension particles.

Numerous investigations on friction and wear behavior of conventional APS coatings with addition of TiO_2, ZrO_2, and Cr_2O_3 have been conducted [13-18]. Wang et al. [3] revealed that dry sliding wear resistance in mild steel coated by

APS with nanostructure Al_2O_3–$13TiO_2$ exhibited four times greater wear resistance than samples coated with conventional powder. Fervel et al. [17] found that dry sliding wear resistance was higher in Al_2O_3-$40TiO_2$ than in Al_2O_3-$13TiO_2$. Vargas et al. [18] investigated Al_2O_3-$13TiO_2$ and Al_2O_3-$43TiO_2$ coatings obtained by APS and concluded that wear resistance was heavily influenced by hardness more than toughness. Sathish et al. [8] evaluated the dry sliding wear of Al_2O_3-$13TiO_2$ obtained by APS from a nanopowder and detected an excellent wear resistance which could be attributed to a lower porosity and higher adhesion strength.

However, no attempts have been made on the development of wear resistance of coatings obtained by suspension plasma spraying. Thus, it is necessary to elucidate the influence of some issues of the suspension plasma spraying process such as the reduction of particle size and different levels of TiO_2 in the coatings wear resistance. In this work, the tribological responses of alumina and alumina-titania near-nanometric coatings obtained by SPS have been investigated. Differences in friction and sliding wear behavior are associated with microstructural and mechanical parameters.

2. Experimental Procedure

2.1 Materials

Two commercial nanometric powders were used to prepare the coating deposition suspension: AKP30 α-Al_2O_3 supplied by Sumitomo Chemical Corp. (Tokyo, Japan) and K2300 TiO_2 rutile produced by Kronos (Leverkusen,

Germany) respectively. Suspensions with an ethanol-base and different compositions of TiO_2 powder were fabricated under ultrasonic and magnetic stirring. Composition and mass percentages of each coating are detailed in Table 1.

A carbon steel disc (AISI 1038) with a 50 mm diameter was used as a substrate in the coating deposition. Before the spraying process, substrate samples were polished down to 0.07 µm with SiC papers and diamond slurries, and cleaned with ethanol. Substrate samples were pre-heated to an average surface temperature of 250 ºC for 40 *s* to enhance coating adhesion.

2.2 Coating deposition

Coating deposition was performed by SPS technique, with a plasma equipment model Multi Coat, a F4-MB (Sulzer-Metco,), a 6 mm internal diameter anode and a mechanical injector specifically built for suspension in by the Science of Ceramic Processing and Surface Treatments (CPCTS) (Université de Limoges, France). Nanometric powder suspensions were injected with a 150 µm internal diameter injector through the plasma flow. Suspension momentum density was controlled by adjusting the pressure in the suspension containers upon penetration within the plasma flow. Plasma mass enthalpy remained at the same level for all coating processes. Plasma spraying process parameters used for coating deposition are listed in Table 2.

2.3 Characterization

Crystalline phase composition of nanoparticles present in powders was tested by X-ray diffraction (*XRD*). Diffractograms were obtained using a Bruker Theta model D8 Advance diffractometer with CuKα radiation (λ=0.154056 nm). The generator settings were 40kV and 30mA. The *XRD* dates were collected by a diffractometer with Bragg Brentano (θ/θ) geometry, in a 2θ range of 20-90˚ with a step width of 0.015˚ and a counting time of 2 s/step. A PSD (VANTEK, BRUKER) solid state detector was used.

Powder morphologies and coating fractures were observed by field emission scanning electron microscopy (*FESEM*, JEOL 7400F). Coating microstructure was observed in cross-sectioned samples by a scanning electron microscopy (*SEM*, JEOL SM6300) connected to an energy dispersive X-ray microanalysis (*EDX*) instrument. Coating void contents in samples were not determined due to a lack of adequate protocols [19].

2.4 Sliding wear test

Tribological tests were carried out under dry sliding conditions by a tribometer pin-on-disc (ball on disc configuration) manufactured by CSM Instruments (Lausanne, Switzerland), according to ASTM wear testing standards G99-03 [20]. All tests were conducted in a dried mode, and wear debris were removed constantly from the wear track by compressed air. A ball of α-Al_2O_3 with a 6 mm radius and a hardness of 2400 HV_{10}, produced by GMS Ball Co Ltd was used as counter material. The tests were performed with the following parameters:

contact loads of 2 N, sliding speed of 0.1 m/s, sliding distance of 1200 m and a wear track radius of 12.5 mm. Environmental conditions were controlled in all tests to a temperature of 23 ± 2˚C and 60 ± 2% relative humidity. In order to obtain enough representative values of each investigated parameter, a series of three tests for each material was carried out. Wear track and cross-sectioned wear surfaces were examined by scanning electron microscopy, SEM (JEOL SM6300) and energy-dispersing X-ray analysis (EDX).

Wear volume loss, V_{wear}, was determined from the wear track profile. Track profiles were measured using a Taylor Hobson (Leicester, England) surface profiler equipped with a diamond tip of 5 µm radius. Ten random measurements were obtained from each wear track and averaged after an adjustment of 20%, i.e. the highest and the lowest values were discarded. The wear rate, K_v, was calculated according to the wear formula by Lancaster [21], as shown in Eq. (1)

$$k_v = \frac{V_{wear}}{F_N \times S} \quad \left[mm^3 N^{-1} m^{-1} \right] \qquad (1)$$

where V_{wear} is the volume lost expressed in mm^3. F_N is the normal load applied in N and S is the sliding distance in m.

3. Results and discussion

3.1. Coating Architecture

SEM micrographs of cross-sectioned SPS alumina and alumina-titania coatings are shown in Fig.1. SEM micrograph observations revealed no clear evidence of real microstructure in *SPS* samples. This can be attributed to:

i) coatings presented a finer microstructure,

ii) limited resolution in SEM,

iii) contamination during the metallographic step due to the appearance of voids from particles which were removed and re-introduced to the surface during the polishing process.

Therefore, SEM micrographs of *SPS* coating samples were only used to estimate coating thickness, as shown in Table 3.

Data shown in Table 3 revealed an inverse relation between TiO_2 composition and coating thickness. Hence, an increase in addition of TiO_2 reduced coating thickness. This relation can be associated with the lower melting point and specific heat of TiO_2 in comparison to Al_2O_3 [13,17,22].

APS data samples presented by Pawlowski L. et al. [9] and Xiao D. et al. [10] were compared with SPS samples obtained in this study. *SPS* samples showed a reduction in coating thickness compared to *APS* samples. A direct relation between coating thickness, solid particle mass ratio and feedstock size particle, was evident in *SPS* samples, which is consistent with Fauchais P. et al. [22] observations.

SEM/BSE micrograph, Fig. 2, shows element distribution for alumina-titania coatings microstructure. In general, microstructure observations revealed a layer with splat morphology in deposits. Contrast obtained by back scattered electronic technique, BSE, suggests dark particles represent rich aluminum areas whilst

light grey layers are indicative of heavier elements such as titanium. Cracks in coating microstructure (intra-lamellar failures) and delamination (inter-lamellar failures) were not found at this image resolution. In addition, cohesion between splats was excellent.

As shown in Fig. 2, *SPS* coating samples exhibit a finer microstructure than *APS* samples. Also, the thickness of splat layers in *SPS* coating samples was less than 100 nm. In this case, projection with the SPS technique produced splats on the same scale as the initial feedstock size (300-400 nm). The near- nanometric structure is one of the most important characteristics in wear behavior in these materials. This will be discussed later.

Fracture morphology of *SPS* coatings was observed by FESEM micrographs. Coating microstructure architecture throughout the fracture is shown in Fig.3. Microstructure architecture included: well molten particles which formed flattened lamellae, unmelted particles from the initial feedstock and molten particles smaller than the initial feedstock. These smaller molten particles had enough time to re-solidify but did not reach the required speed to flatten against the substrate. This structure was also found in other investigations [12,23,24].

Finally, SPS coatings showed the same size scale as the initial scale feedstock (submicrometer) and a reduction of some particles to near-nanometric scale. This improvement in coating microstructure was related to the accurate spraying conditions selected for the SPS process which achieved a perfectly solidified coating.

3.2 Friction coefficient

Friction coefficient, μ, is the ratio between friction force and normal force. In a tribometer with ball on disc configuration, friction force is continuously measured by a load cell with a piezoelectric transductor positioned over the loading arm. Friction coefficient evolution is usually separated into two different regions: running-in and steady state [17]. The first stage is related to the running of materials against themselves. In the second stage it is assumed that part and counterpart form a system [25].

Friction coefficient evolution, as a function of sliding distance for all tested materials, is reported in Fig. 4. In general, first observations show that the addition of TiO_2 to coatings reduces the friction coefficient, except in the case of material AT13. Moreover, regular friction coefficient behavior is observed in materials with the addition of TiO_2, while for material AT it becomes irregular.

Friction coefficient behaviors of evaluated coatings were divided into two groups for a better understanding of the friction phenomenon involved. Materials were separated into the first group AT y AT13 and second group AT25 y AT40.

In the first group, the running-in state was extended in material without TiO_2 (up to 900 m sliding distance), whilst with the inclusion of 13%TiO_2 this effect reduced (up to 700 m sliding distance). Although both materials showed an increase in friction coefficient, the evolution was irregular in AT. This behavior is determined by an abrupt removal of fragments from material, which constitutes the tribopair, and produces an increase in plowing and third body in the contact

zone [26]. Irregularities found in AT material can be attributed to a larger contribution of third body which still remained and circulated in the contact area. As sliding continues, steady state is reached in both materials, up to 1200 meters of sliding distance. This behavior can be justified with the multi-asperity contacts theory by Zhang et al. [27,28] which suggests that friction coefficient evolution is due to three components: adhesion, asperity plowing and debris plowing.

Materials in the second group showed a similar friction behavior. This is characterized by a reduction of running-in state extension up to 400m of sliding distance in comparison with the first group. This behavior can be attributed to asperities plowing effect of hard coatings to soft counter material surfaces and a small contribution of wear debris. As sliding continues, steady state is reached in both materials and maintained until the end of the test with a constant friction coefficient. Friction behavior in these materials is dominated by asperity polishing and reduction in wear debris generation.

Some research studies provided information about friction coefficient values in Al_2O_3 and Al_2O_3-13TiO_2 APS coatings [15,17,25,29], but not enough information was found for Al_2O_3-25TiO_2 and Al_2O_3-40TiO_2 [15,30].

The addition of TiO_2 reduced the friction coefficient value in evaluated coatings, except for the AT13 combination. Although, AT13 did not present a reduction in friction coefficient, its value is less than the value presented by Guesama et al. and Bolelli et al. for micrometric coatings [25,29]. Material AT25 showed the lowest friction coefficient in respect to material AT, which means a reduction of

62%. It should be noted that this friction coefficient value is less than the values reported by Dejang et al. [15] and Fervel et al. [17] in sub-micrometric and nanostructure coatings.

3.3. Wear characteristic

Wear resistance is not a material property, wear mechanisms and the associated volumetric wear rate, K_v, depend critically on the precise conditions to which they are subjected [31].

Fig. 5 shows wear rate results in the function of TiO_2 compositions for all tested materials. First observations indicate an inverse relation between wear rate and TiO_2 composition. Wear rates decrease as wt.% of TiO_2 increase, behavior which is consistent with results reported by Fervel et al., Bolelli et al. and Ahn et al. [17,29,32].

The excellent response in wear resistance from the addition of TiO_2 can be attributed to the effect of titania in improving the binding of sprayed alumina particles in the coating, which results in the reduction of wear of particles or lamellae in the coating [13]. Indeed, an increase in TiO_2 composition, as small as 13%, AT13 allows an increase of 1.5 times in wear resistance compared with material without TiO_2, AT.

The best response to dry sliding wear resistance is shown by material AT40. Indeed, AT40 shows an increase of 2.6 times in wear resistance than material AT. Several authors [14,33,34] proposed that the wear of brittle ceramics is proportional to fracture toughness on the basis that wear occurs by brittle

cracking. Furthermore, an increase in TiO_2 addition forms a denser splat layer, which allows an increase in fracture toughness and a subsequent increase in wear resistance.

3.4 Wear surface observation

Wear is an extremely complex process with many influencing factors. In certain cases, one or more factors will dominate the wear resistance of the materials, but they change as conditions change [3]. Several wear mechanisms, such as: abrasion, adhesion, micro-fractures and delamination (separated or combined) contribute to the wear damage in ceramic-ceramic sliding contact [35].

SEM micrographs of wear tracks are shown in Fig.6. Different levels of surface damage were observed. Pattern wear damages observed were consistent with wear rate behaviors presented by coating samples. Thus, material without the addition of TiO_2, AT, shows the worst damage, whilst AT13 and AT25 are in a previously damaged state and finally AT40 shows almost no wear signs on the surface.

Material AT, Fig. 6a, shows the worst pattern damage due to the coexistence of several wear mechanisms. The wear track shows the appearance of a compact wear debris layer adhered to the surface. The splats of Al_2O_3 coatings are detached by brittle fracture [18,36] and debris appeared in the subsequent fragmentation of these splats. Wear debris are then embedded or pulled out of the wear track creating a tribological layer, abrasion mechanism takes place upon the tribolayer at the same time that brittle fracture appears. The debris, still

remained in the contact surface and, constitutes a "third body" in the sliding system and influences the contact stresses and wear [37]. In addition, grooving, micro-fracture and some holes are observed in the tribolayer [38] due to removal of particles, as a product of the wear process, Fig 6 a.

The improvement in wear resistance of material AT13 in comparison with material AT was supported by the wear damage patterns. Wear track of material AT13 showed an irregular tribolayer, areas where splats were plastically deformed and other areas with wear debris attached. Wear debris were removed from the surface due to the abrasion wear mechanism, although less than in material AT due to the best bonding strength between splats in this coating. As movement continues, adhesion wear mechanism appears and wear debris are adhered to the surface, where they accumulate in holes and abrasion grooves, to finally create the tribolayer. In addition, several cracks perpendicular to the sliding movement were observed and propagated through deformed areas [11]. Hence, TiO_2 presence in coatings increases fracture toughness and reduces the strain hardening component.

Dry sliding wear resistance was remarkably improved in materials AT25 and AT40. Wear track observation indicates a damage stage prior to material AT13, which is in accordance with obtained wear rates data. However, material AT25 shows worse pattern damage than material AT40. Wear track in material AT25 shows asperity deformation, plowing in sliding direction, a few holes due to particles being removed and plastically deformed splats. There is no evidence of a consistent tribolayer although wear debris formation is observed in the damage

surface. Wear track of material AT40 shows a small presence of plastically deformed splats and an incipient abrasion mechanism which is evidence of the excellent wear resistance of this material.

Near-nanometric structures obtained by SPS in these coatings lead to splats, melting particles, partial melting particles and defects that involve the microstructure remained in the same size range. Furthermore, an increase in inter-lamellar cohesion and wear resistance is directly linked to reduction in defect sizes. The addition of TiO_2 to coatings provided a better structure densification and ductility which enhanced dry sliding wear resistance. Extraction of particles from wear surfaces becomes difficult as microstructures become denser and an increase in ductility produces more plastic flow, which inhibits the wear debris appearance. Finally, the greatest improvement in the dry sliding wear resistance of these coatings is achieved by the combination of near-nanometric structure and the addition of TiO_2.

4. Conclusions.

Friction and wear behavior of alumina and alumina-titania coatings fabricated by SPS was studied in a ball-on-disk tribometer.

- It has been determined that the microstructure of coatings obtained by means of SPS remain on the same size scale than the initial feedstock, presenting at the same time some particles where the microstructure is reduced to near-nanometric scale. The accurate definition of spraying conditions plays an important role in the final result.

- A noticeable reduction in friction coefficient was found in coatings with the addition of more than 13 wt.% of titania. An important reduction of 62% in the friction coefficient value was found in coatings with 25 wt.% of titania.

- The wear rate is inversely affected by the wt.% of TiO_2 in coatings. The addition of 40 %wt. titania increases dry sliding wear resistance 2.6 times compared to the 100 %wt. alumina coating.

- The excellent sliding wear resistance of coatings was attributed to the combination of adding titania and the near-nanometric structure obtained by SPS. Titania addition provided a better structure densification and ductility while the reduction in grain size reduces defects, splats and melting particles.

- The marked differences found in wear resistance coatings are corroborated by damage patterns observed in wear tracks. The wear mechanism is controlled by: plastic deformation, asperity deformation, abrasion in the sliding movement, particles pulled out and tribolayer formation.

Acknowledgments

The authors wish to thank for the Spanish Ministery of Economy and Competitiviness (MAT2012-38364-C03), the Autonomous Government of Valencia funding for the stay in SPCTS-UMR CNRS (France) and French FCENANOSURF consortium that was granted by the French Ministry and Industry and local governments of Région Centre and Région Limousin.

References

[1] L. Pawlowsky, Thermal spraying techniques, The Science and Engineering of Thermal Spray Coatings, John Wiley & Sons, New York, 1995.

[2] Th. Lampe, S. Eisenberg, E.R. Cabeo, Plasma surface engineering in the automotive industry –trends and future prospective, Surface and Coating Technology 174–175 (2003) pp.1-7.

[3] Y. Wang, S. Jiang, M. Wang, S. Wang, T.D. Xiao, P.R. Strutt, Abrasive wear characteristics of plasma sprayed nanostructured alumina/titania coatings, Wear 237 (2000) pp.176–185.

[4] L.T. Kabacoff, Nanoceramic coatings exhibit much higher toughness and wear resistance than conventional coatings, The AMPITAC News letter, 6-1 (2002) pp. 37–42.

[5] M. Wang, L.L. Shaw, Effects of the powder manufacturing method on microstructure and wear performance of plasma sprayed alumina-titania coatings, Surface and Coatings Technology 202 (2007) pp. 34-44.

[6] L.L.Shaw, D. Goberman, R. Ren, M.Gell, S. Jing, Y. Wang, T.D. Xiao, P.R. Strutt, The dependency of microstructure and properties of nanostructured coatings on plasma spray conditions, Surface and Coatings Technology 130 (2000) pp. 1-8.

[7] N. B. Dahotre, S. Nayak, Nanocoatings for engine application, Surface and Coatings Technology 194 (2005) pp- 58-67.

[8] S. Sathish, M. Geetha, S.T. Aruna, N. Balaji, K.S. Rajam, R. Asokamani, Sliding wear behavior of plasma sprayed nanoceramic coatings for biomedical applications, Wear 271 (2011) pp.934–941.

[9] L. Pawlowski, “Finely grained nanometric and submicrometric coatings by thermal sparing: A review”, Surface and Coating Technology 202 (2008) pp. 4318-4328.

[10] D. Xiao, Y. Wang, P. Strutt, “Fabrication and evaluation of plasma sprayed nanostructured alumina-titania coatings with superior properties”, Materials Science and Engineering 301 (2001) pp. 80-89.

[11] S.C. Tjong, H. Chen, Nanocrystalline Materials and Coatings, Materials and Science Engineering R 45 (2004) pp. 1-88.

[12] P. Fauchais, G. Montavon, G. Bertrand, From powders to thermally sprayed coatings, Journal of Thermal and Spray Technology 19 (2010) pp. 56-80.

[13] K. Ramachandran, V. Selvajaran, P.V. Ananthapadmanabhan, K.P. Sreekumar, Microstructure, adhesion, micro hardness, abrasive wear resistance and electrical resistivity of the plasma sprayed alumina and alumina-titania coatings, Thin Solid Films 315 (1998) pp.144-152.

[14] S.W. Lee, C. Morillo, J. Lira-Olivares, S.H. Kim, T. Sekino, K. Niihara, B.J. Hockey, Tribological and microstructural analysis of $Al_2O_3/13TiO_2$ nanocomposites to use in femoral head of hip replacement, Wear 225 (2003) pp. 1040- 1044.

[15] N. Dejang, A. Watcharapasorn, S. Wirojupatump, P. Niranatlumpong, S. Jiansirisomboon, Fabrication and properties of plasma-sprayed Al_2O_3/TiO_2 composite coatings: A role of nano-sized TiO_2 addition, Surface and Coating Technology 204 (2010) pp.1651-1657.

[16] S. Yimaz, An evaluation of plasma sprayed coatings based on Al_2O_3 and Al2O3-13wt% TiO2 with bond coat on pure titanium substrate, Ceramics International 35 (2009) pp.2017-2022.

[17] V. Fervel, B. Normand, C. Coddet, Tribological behavior of plasma sprayed Al_2O_3- based cermet coatings, Wear (1999) pp.70-77.

[18] F. Vargas, H. Ageorges, P. Fauchais, M.E.López, Mechanical and a tribological performance of Al_2O_3 coatings elaborated by flame and plasma spraying, Surf. Coat. Technol. 205 (2010) 1132-1136.

[19] A. Bacciochini, J. Ilavsky, G. Montavon, A. Denoirjean, F. Ben-ettouil, S. Valette, P. Fauchais, K. Wittmann-teneze, Quantification of void network architectures of suspension plasma-sprayed (SPS) yttria-stabilized zirconia (YSZ) coatings using Ultra-small-angle X-ray scattering (USAXS) Materials Science Engineering 528 (2010) pp.91-102.

[20] ASTM G99-03, Standard Test Method for Wear Testing With a Pin-on-disc Apparatus, ASTM Annual Book of Standards, vol. 03.02, West Conshohocken, PA, 2003

[21] K. Lancaster, The influence of substrate hardness on the formation and endurance of molybdenum disulphide films, Wear 10 (1967) pp.103-107

[22] P. Fauchais, V. Rat, C. Delbos, J. Fazilleau, J. F. Coudert, T. Chartier, and L. Bianchi, “Understanding of suspension plasma spraying of finely structured coatings for SOFC”, IEEE Trans. on Plasma Science 33(2) (2005) pp.920-930.]

[23] G. Darut, F. Ben- Ettouli, A. Denoirjean, G. Montavon, H. Ageourges, P. Fauchais, Dry sliding behavior of sub-micrometer-sized suspension plasma sprayed ceramic oxide coatings, Journal of Thermal Spray Technology 19 (2010) pp.275-285.

[24] O. Tingaud, A. Bacciochini, G. Montavon, A. Denoirjean, P. Fauchais, Suspension DC plasma spraying of thick finely-structured ceramic coatings: Process manufacturing mechanisms, Surface Coatings Technology 203 (2009) pp.2157-2161.

[25] S. Guesama, M. Bounazef, P. Nardin, T. Sahraoui, Wear behavior of alumina-titania coatings: analysis of process and parameters, Ceramics International 32 (2006) pp.13-19.

[26] L. Espinosa-Fernández, A. Borrell, M.D. Salvador, C.F. Gutierrez-Gonzalez, Sliding wear behavior of WC–Co–Cr_3C_2–VC composites fabricated by conventional and non-conventional techniques, Wear 307 (2013) pp.60–67.

[27] J. Zhang, F.A. Moslehy, S.L. Rice, A model for friction in quasi-steady-state. Part I. Derivation, Wear 149 (1991) pp.1-12.

[28] J. Zhang, F.A. Moslehy, S.L. Rice, A model for friction in quasi-steady-state sliding Part II. Numerical results and discussion, Wear 149 (1991) pp.13-25.

[29] G. Bolelli, V. Cannilo, L. Lusvarghi, T. Manfredini, Wear behaviour of thermally sprayed ceramic oxide coatings, Wear 261 (2006) pp.1298-1315.

[30] B. Normand, V. Fervel, C. Coddet, V. Nikitine, Tribological properties of plasma sprayed alumina-titania coatings:next term role and control of the microstructure, Surface Coatings Technology 123 (2000) pp.278-287.

[31] I. Hutchings, Tribology: Friction and Wear of Engineering Materials, Materials & Design 13 (1992) pp.187.

[32] J. Ahn, B. Hwang, E.P. Song, S. Lee, N.J. Kim, Correlation of microstructure and wear resistance of Al_2O_3-TiO_2 coatings plasma sprayed with nanopowders, Metallurgical and materials transactions 37A (2006) pp.1851-1860.

[33] L.C. Erickson, H.M. Hawthorne, T. Troczynski, Correlations between microstructural parameters, micromechanical properties and wear resistance of plasma sprayed ceramic coatings, Wear 250 (2001) pp. 569-575.

[34] E.P. Song, J. Ahn, S. Lee, N.J. Kim, Microstructure and wear resistance of nanostructured Al_2O_3-8wt.%TiO_2 coatings plasma-sprayed with nanopowders, Surface and Coatings Technology 201 (2006) pp.1309-1315.

[35] Handbook of Thermal Spray Technology, ASM International, Materials Park, OH, USA, pp.171.

[36] G.W. Stachowiack, A. Batchelor, Engineering Tribology handbook (Butterworth Heinemann), chapter 16 pp.650.

[37] T.E. Fischer, Z. Zhu, H. Kim, D.S. Shin, Genesis and role of wear debris in sliding wear of ceramics, Wear 245 (2000) pp.53-60.

[38] R.S. Lima, C. Moureau, B.R. Marple, HVOF-Sprayed coatings engineered from mixtures of nanostructured and submicron Al_2O_3-TiO_2 powders: an enhanced wear performance, Journal of Thermal Spray Technology, 16 (2007) pp.866.

Table
Click here to download Table: Table 1 Suspensions characteristic.docx

Table 1 Suspensions characteristic.

Designation	**AT**		**AT13**		**AT25**		**AT40**	
Powder type	Al_2O_3	TiO_2	Al_2O_3	TiO_2	Al_2O_3	TiO_2	Al_2O_3	TiO_2
Material/Powder (wt.%)	100	-	87	13	75	25	40	60
d_{50} of particle size distribution (nm)	300							
Liquid phase	Et-OH (99.5%)							
Powder/Suspension (wt.%)	10							
Dispersant/powder (wt.%)	2.0							

Table
Click here to download Table: Table 2 Plasma spraying process parameters.docx

Table 2 Plasma spraying process parameters.

Primary plasma gas flow rate, (slpm*)	40 (Ar)
Secondary plasma gas flow rate, (slpm*)	20 (He)
Arc current intensity, (A)	600
Torch scan velocity, ($m\text{-}s^{-1}$)	1
Scanning step, ($mm\text{-}pass^{-1}$)	10
Spray distance, (mm)	30
Spraying time, (min)	2

* slpm: standard litre per minute.

Table
Click here to download Table: Table 3 Thickness of alumina and alumina.docx

Table 3 Thickness of alumina and alumina-titania coatings.

	AT	**AT13**	**AT25**	**AT40**
Thickness, (µm)	21,1 ± 0,8	16,3 ± 9,3	16,6 ± 4,9	15,9 ± 1,8

Figure
Click here to download Figure: Figure. 1 SEM micrographs.docx

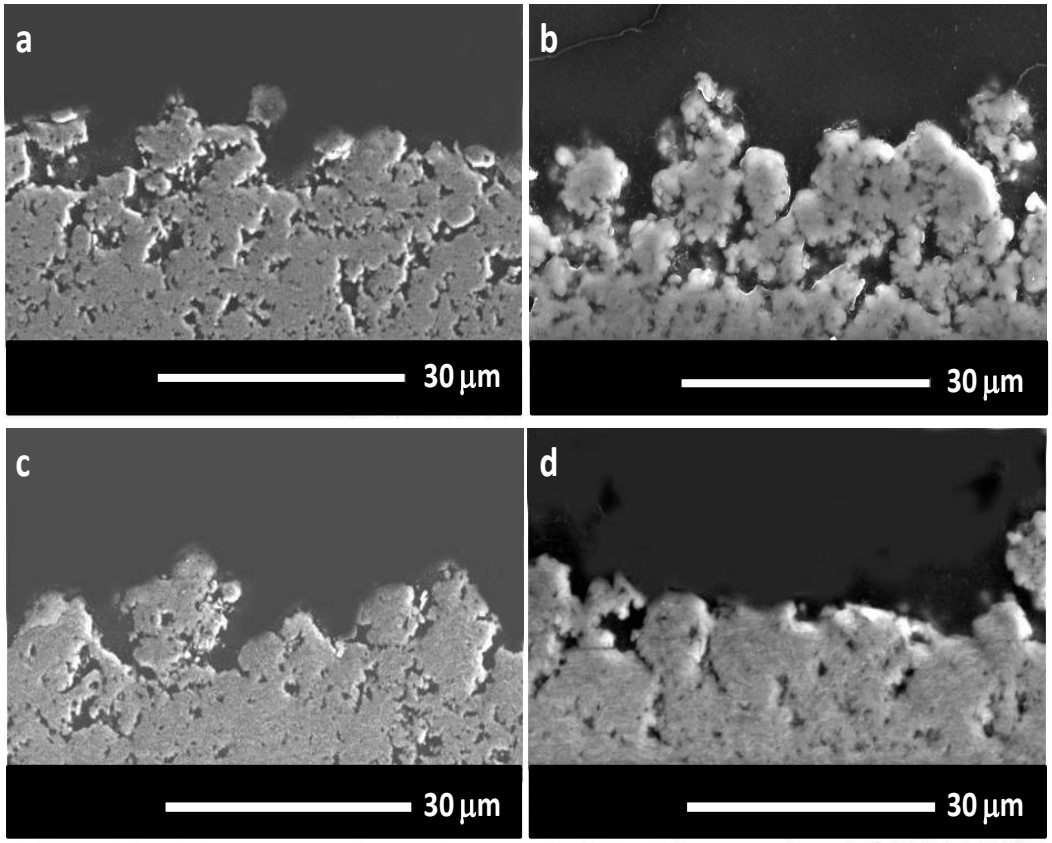

Figure. 1 SEM micrographs of alumina and alumina-titania coatings cross-sections: (a) AT, (b) AT13, (c) AT25 and (d) AT40.

Figure
Click here to download Figure: Figure. 2 SEM_BSE micrographs.docx

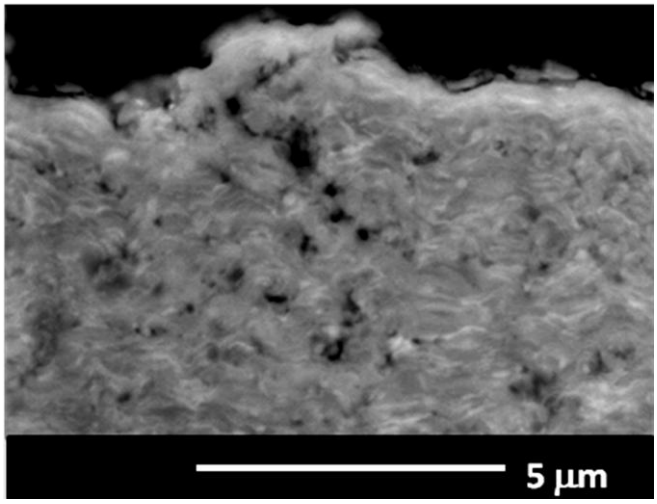

Figure. 2 SEM/BSE micrograph of AT40 coating cross-section.

Figure
Click here to download Figure: Figure. 3 FESEM micrograph.docx

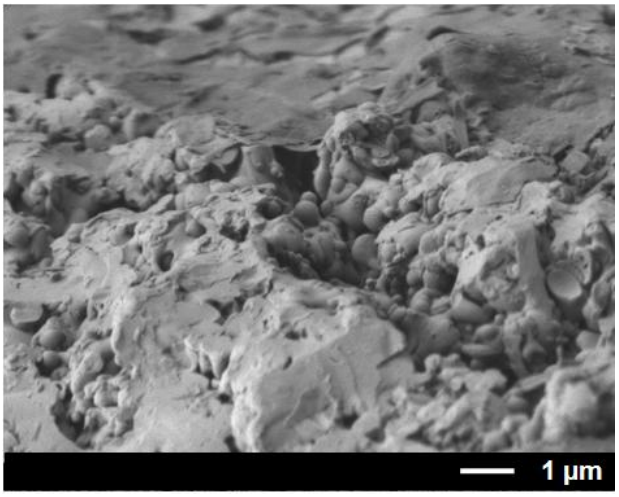

Figure. 3 FESEM micrograph of fracture surface in AT coating.

Figure
Click here to download Figure: Figure. 4 Friction coefficients.docx

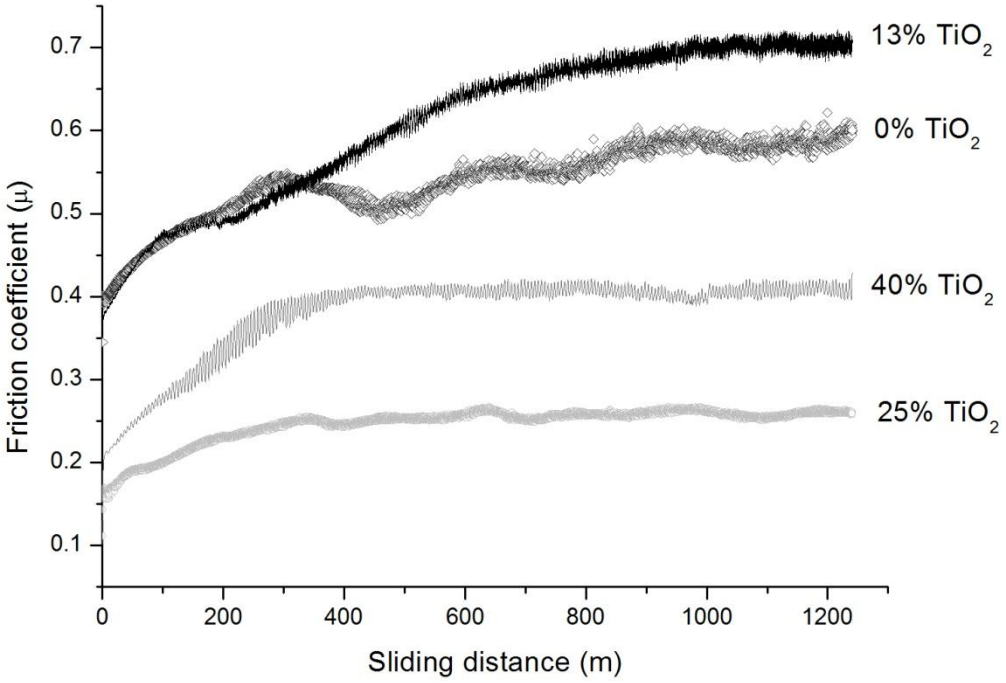

Figure. 4 Friction coefficients evolution with sliding distance for studied coatings.

Figure
Click here to download Figure: Figure. 5 wear rate.docx

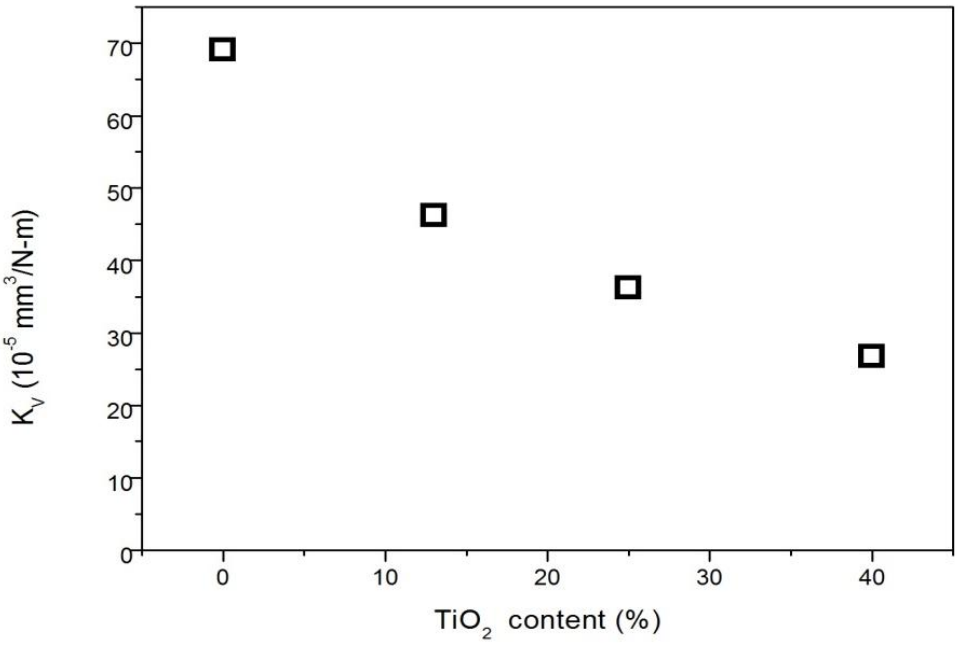

Figure. 5 Wear rate as a function of TiO_2 content of the tested coatings.

Figure
Click here to download Figure: Figure. 6 SEM micrographs.docx

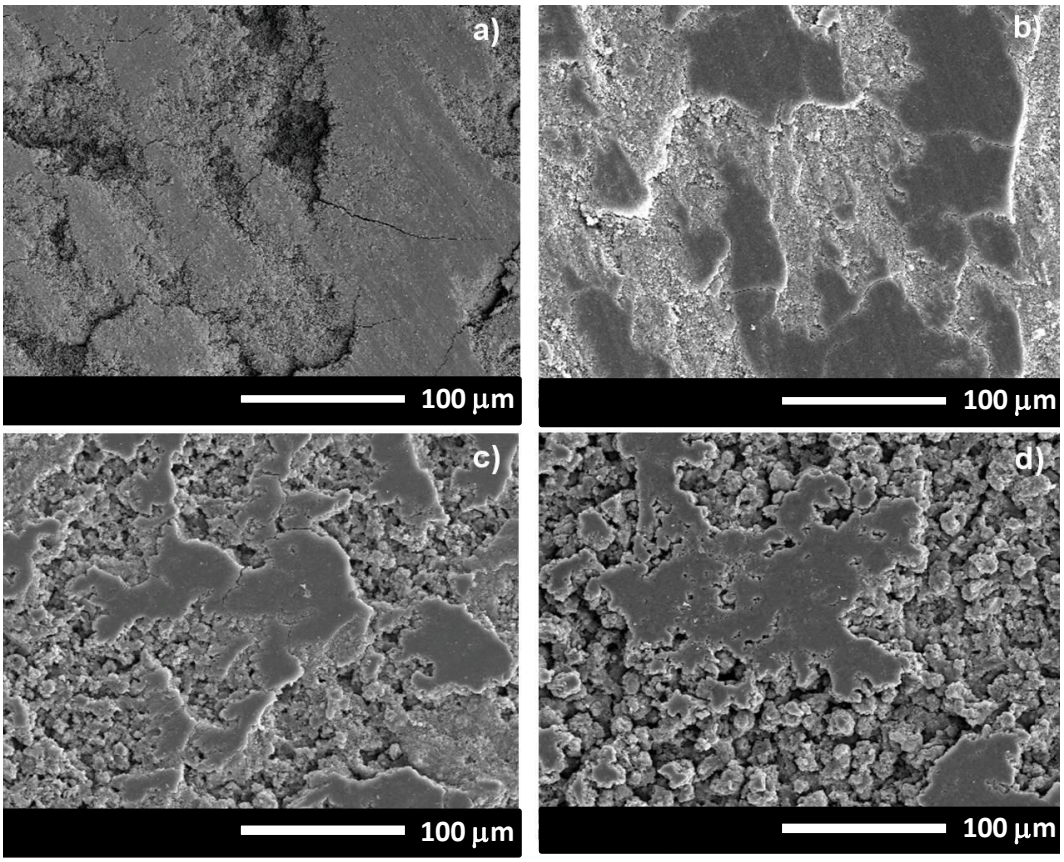

Figure. 6 SEM micrographs of wear tracks of tested coatings: (a) AT, (b) AT13, (c) AT25 and (d) AT40.